Planta (2012) 235:39–52
DOI 10.1007/s00425-011-1481-1

ORIGINAL ARTICLE

Wax crystal-sparse leaf2, a rice homologue of WAX2/GL1, is involved in synthesis of leaf cuticular wax

Bigang Mao · Zhijun Cheng · Cailin Lei · Fenghua Xu · Suwei Gao · Yulong Ren · Jiulin Wang · Xin Zhang · Jie Wang · Fuqing Wu · Xiuping Guo · Xiaolu Liu · Chuanyin Wu · Haiyang Wang · Jianmin Wan

Received: 29 April 2011 / Accepted: 7 July 2011 / Published online: 2 August 2011

Abstract Epicuticular wax in plants limits non-stomatal water loss, inhibits postgenital organ fusion, protects plants against damage from UV radiation and imposes a physical barrier against pathogen infection. Here, we give a detailed description of the genetic, physiological and morphological consequences of a mutation in the rice gene *WSL2*, based on a comparison between the wild-type and an EMS mutant. The mutant's leaf cuticle membrane is thicker and less organized than that of the wild type, and its total wax content is diminished by ~80%. The mutant is also more sensitive to drought stress. *WSL2* was isolated by positional cloning, and was shown to encode a homologue of the *Arabidopsis thaliana* genes *CER3/WAX2/YRE/FLP1* and the maize gene *GL1*. It is expressed throughout the plant, except in the root. A transient assay carried out in both *A. thaliana* and rice protoplasts showed that the gene product is deposited in the endoplasmic reticulum. An analysis of the overall composition of the wax revealed that the mutant produces a substantially reduced quantity of C22–C32 fatty acids, which suggests that the function of WSL2 is associated with the elongation of very long-chain fatty acids.

Keywords Cuticular wax · Rice (*Oryza sativa* L.) · Verylong-chain fatty acid (VLCFA) · *Wax crystal-sparse leaf2*

Abbreviations

CER	ECERIFERUM
EMS	Ethyl methane sulfonate
FAE	Fatty acid elongase
GC–MS	Gas chromatography–mass spectrometry
SEM	Scanning electron microscope
TEM	Transmission electron microscope
VLCFA	Verylong-chain fatty acid
WSL2	Wax crystal-sparse leaf2

Introduction

Among the various functions of the cuticle, a structure which covers the aerial surface of terrestrial plants, are the prevention of non-stomatal water loss, the inhibition of organ fusion during development (Sieber et al. 2000; Raven and Edwards 2004), protection from UV radiation damage (Barnes et al. 1996) and the imposition of a physical barrier against infection by bacterial and fungal pathogens (Jenks et al. 1994; Riederer 2006). The two major components of the cuticle are the hydroxyl and hydroxyl-epoxy fatty acid polyester cutin, and cuticular wax, which is a complex mixture of straight chain C20–C60 aliphatics. A typical cuticle has an outer coating of

B. G. Mao, Z. J. Cheng and C. L. Lei contributed equally to this work.

Electronic supplementary material The online version of this article (doi:10.1007/s00425-011-1481-1) contains supplementary material, which is available to authorized users.

B. Mao · Z. Cheng · C. Lei · F. Xu · S. Gao · Jiulin Wang · X. Zhang · Jie Wang · F. Wu · X. Guo · X. Liu · C. Wu · H. Wang · J. Wan (✉)
National Key Facility for Crop Gene Resources and Genetic Improvement, Institute of Crop Science, Chinese Academy of Agriculture Sciences, Beijing 100081, China
e-mail: wanjm@njau.edu.cn; wanjm@caas.net.cn

Y. Ren · J. Wan
National Key Laboratory for Crop Genetics and Germplasm Enhancement, Jiangsu Plant Gene Engineering Research Center, Nanjing Agricultural University, Nanjing 210095, China

cuticular wax (a mixture of long-chain lipids (Walton 1990), a thick electron-translucent middle layer (the "cuticle proper") and an electron-dense cuticular layer (Taiz and Zeiger 1998). Both cutin and cuticular wax are synthesized in the epidermal cells. In *Arabidopsis thaliana*, the synthesis of cuticular wax derives from the elongation of saturated C16 and C18 fatty acids, which is catalysed by a multi-enzyme fatty acid elongase (FAE) complex (Joubes et al. 2008; Kunst and Samuels 2009). The resulting precursors are subsequently modified into a range of aldehydes, alkanes, secondary alcohols and ketones via the alkane pathway or into primary alcohols and wax esters via the primary alcohol pathway (Samuels et al. 2008).

Many of the wax-related genes cloned so far in *A. thaliana* appear to be involved in the synthesis of long-chain fatty acid wax precursors. FATB, for example, has a role in the supply of saturated fatty acids for the synthesis of VLCFAs in the plastid (Bonaventure et al. 2003). LACS2 and LACS1/CER8 are primarily responsible for the CoA esterification of fatty acids en route to wax synthesis (Schnurr et al. 2004; Lu et al. 2009). CER6 (Fiebig et al. 2000) and CER10 (Zheng et al. 2005) are both targeted to the endoplasmic reticulum (ER), where they show, respectively, β-ketoacyl-CoA synthase and enoyl-CoA reductase activity. AtKCR1 is a homologue of a yeast enzyme which catalyses an early step in the elongation of VLCFAs, and functions as a β-ketoacyl-CoA reductase (Beaudoin et al. 2009). PAS2, which encodes a β-hydroxyacyl-CoA dehydratase, is considered essential for normal plant development (Bach et al. 2008). Each of the four latter enzymes is an important component of the FAE complex (Kunst and Samuels 2009). The fatty acyl-CoA reductase CER4 catalyses the production of primary alcohols from VLCFA acyl-CoA (Rowland et al. 2006) and can also act as the substrate for the synthesis of alkyl esters by wax synthase WSD1 (Li et al. 2008). Meanwhile, MAH1, a mid-chain alkane hydroxylase, catalyses the oxidization of alkanes to form secondary alcohols and ketones (Greer et al. 2007).

Mutants of the *A. thaliana* genes *CER3*, *WAX2*, *YRE* and *FLP1* (multiple alleles, hereafter this gene will be referred to as *WAX2*) are all associated with major loss in the amount of wax produced (Ariizumi et al. 2003; Chen et al. 2003; Kurata et al. 2003; Rowland et al. 2007), but how they participate in wax synthesis remains unclear. In the *wax2* mutant, the extent of the reduction is close to 80%, and except for the C30 primary alcohols, the presence of all the other components (alkanes, ketones, aldehydes and secondary alcohols) is markedly reduced (Chen et al. 2003). However, in the maize *gl1* mutant (*GL1* is the assumed orthologue of *WAX2*), the dramatic reduction in the presence of aldehydes and alcohols has suggested that GL1 is essential for the elongation process during the synthesis of cuticular wax. Unlike the *wax2* phenotype, however, that of *gl1* does not involve any post-genital fusion or the formation of a somewhat thinner cuticle membrane (Chen et al. 2003; Sturaro et al. 2005). *WAX2* may be regulated at the transcriptional level by the 3′-5′ exoribonuclease CER7 (Hooker et al. 2007).

Here, we describe the characteristics of *wsl2*, a leaf wax-deficient EMS mutant in rice. The leaves of this mutant produce markedly less cuticular wax than the wild type, and the cuticle membrane is substantially altered in form. The mutated gene has been isolated, and shown to be a homologue of *WAX2/GL1*, which are known to play an important role in the synthesis of cuticular wax.

Materials and methods

Plant materials and growth conditions

A rice cuticle wax-deficient mutant (*wsl2*) was identified among a mutagenised population derived by treating the *japonica* landrace Lijiangxintuanheigu (LTH) with 0.6% w/v EMS. The mutant was crossed with the cv. Nanjing11 to construct an F_2 mapping population. A set of 2,017 mutant type F_2 progeny was selected at the four-leaf stage to take forward for fine genetic mapping. For a drought test, 2 week-old seedlings were grown under 28°C, 14 h photoperiod. Grain of LTH, Nanjing11 and the standard *japonica* cultivar Nipponbare and Kitaake were obtained from the Chinese National Key Facility for Crop Gene Resources and Genetic Improvement.

Scanning and transmission electron microscopy

Leaves of 6 week-old seedlings and the lemmas of wild-type and wsl2 plants were air dried (Jenks et al. 1992). Wild-type and wsl2 anthers were fixed for 24 h in 2.5% (v/v) glutaraldehyde (Sigma), rinsed three times for 10 min in distilled water, dehydrated through an ethanol series, fixed in 1% (w/v) osmium tetroxide (Alfa Aesar) for 2 h, rinsed three times for 30 min in 0.1 M sodium phosphate buffer, dehydrated through an acetone series, exchanged for three times with isoamyl acetate (Sigma), and subjected to critical point drying with CO_2. The material was mounted on aluminium stubs and sputter-coated with gold palladium in six 30 s bursts (E-1010 sputter-coater, Hitachi, Tokyo, Japan) in preparation for SEM (Hitachi S-3400N). For TEM, leaf specimens were collected from the middle of the blade between the mid-vein and the leaf margin, fixed in 1% (v/v) glutaraldehyde and 1% (w/v) osmium tetroxide for 1 h at room temperature, dehydrated through an ethanol series, infiltrated and embedded in London Resin White (London Reson Co. Ltd.). A series of 80 nm sections was cut using an Ultracut E ultramicrotome (Leica, Wetzlar,

Germany) and attached to a formvar-coated copper grid (Electron Microscopy Sciences). The sections were air-dried, treated with 2% (v/v) uranyl acetate for 5 min at room temperature and then stained with lead citrate for 3 min viewing with a TEM (Hitachi H-7500).

Chlorophyll efflux and the rate of water loss

Leaf blades of 12 week-old plants were cut into 8 cm lengths and immersed in 80% ethanol. A series of 100 µl aliquots was taken at 1, 2, 4, 6, 8, 10 and 24 h, and subjected to spectrophotometry (absorption measured at 647 and 664 nm) to quantify the amount of chlorophyll leached. The concentration (µM) of chlorophyll in the leachate was given by $7.93 \times A_{664} + 19.53 \times A_{647}$ following Lolle et al. (1997). Leaf water loss rate was assessed from detached leaves of 12 week-old plants. The leaves were initially soaked in water in the dark for 1 h, after which excess water was removed and the leaves returned to the dark. The leaves were thereafter weighed every 30 min (Chen et al. 2003). The experiment comprised three replicates.

Cuticular wax analysis

Cuticular wax was extracted from the leaf and sheath of 12 week-old plants by a 30 s immersion in chloroform at 60°C (Bianchi et al. 1979; Haas et al. 2001). As an internal standard, 20 µg *n*-tetracosane was added to each sample. The solvent was removed by heating to 40°C under nitrogen. The extracted monomers were treated with 100 µl bis-*N*, *N*-(trimethylsilyl) trifluoroacetamide and 100 µl pyridine for 1 h at 70°C to transform hydroxyl containing compounds into their corresponding trimethylsilyl derivatives. The composition of the sample was then analysed using a capillary gas chromatograph equipped with an HP-1MS column (30 m length, inner diameter 0.32 mm, film thickness 0.25 µm) and attached to a mass spectrometer (GCMS-QP2010, Kyoto, Japan). The GC–MS protocol was as follows: injection at 250, 50°C for 2 min, ramped to 200 at 20°C min^{-1}, 2 min at 200°C, ramped to 320 at 2°C min^{-1}, 14 min at 320°C with He supplied at 1.2 ml min^{-1} as the carrier gas. A flame ionization detector was used for quantitative analyses. The quantity of cuticular wax was expressed per unit leaf surface area, with leaf areas measured using a LI-3000C Portable Area Meter (LI-COR Biosciences).

Fine mapping and isolation of *WSL2*

The genomic DNA of the 2,017 F_2 progeny showing the mutant phenotype was subjected to microsatellite analysis (McCouch et al. 2002). A number of de novo indel markers were also developed based on sequence comparisons between the genomic sequences in the critical regions of cv. Nipponbare and the *indica* cv. 9311. Two pairs of PCR primers (cF1/cR1 and cF2/cR2, sequences given in Table S1) were designed to detect *WSL2* transcription. The 8,331 bp genomic DNA fragment containing the entire *WSL2* coding region and its immediate up- and downstream sequence was amplified from LTH genomic DNA using the primer pair WSL2F1/WSL2R1 (sequences given in Table S1). A CloneEZ^{TM} PCR Cloning kit (GenScript Co., Nanjing, China) was used to insert the resulting fragment into *Sma*I digested pCAMBIA1305 to generate the transformation plasmid pWSL2, which was then introduced into *Agrobacterium tumefaciens* strain EHA105 by electroporation, and from there into the *wsl2* mutant, following methods described by Hiei et al. (1994). The presence of the transgene was confirmed using the wsl2-dCAPS assay (primer sequences given in Table S1).

RNA interference suppression of *WSL2*

The construct pCUbi1390-△FAD2 (ubiqutin promoter and a *FAD2* intron inserted into pCAMBIA1390) was used as an RNAi vector (Stoutjesdijk et al. 2002; Wu et al. 2007). Both the anti-sense and sense orientation of a 303 bp fragment (WSL2-A and WSL2-S) from the *Os09g0426800* 3′-UTR was PCR amplified (primer pairs siWSL2F1/siWSL2R1 or siWSL2F2/siWSL2R2, see Table S1), and separately cloned into the *Sac*I or *Sna*BI sites of pCUbi1390-△FAD2 using a CloneEZ^{TM} Enzyme kit (GenScript Co.), to form the transformation construct pUbi-dsRNAiWSL2. The binary plasmid was introduced into *A. tumefaciens* strain EHA105 by electroporation and transformed into cv. Nipponbare, following Hiei et al. (1994).

Bioinformatics

Sequences matching that of WSL2 were identified using the BLAST algorithm and aligned with BioEdit 7.0 software (http://www.mbio.ncsu.edu/bioedit/bioedit.html). A rooted phylogenetic tree was constructed using MEGA v4.0 software (http://www.megasoftware.net/). The robustness of the phylogeny was tested by bootstrapping (1,000 replicates). Transmembrane analysis was performed using TMHMM Server v2.0 (www.cbs.dtu.dk/services/TMHMM/).

RT-PCR, quantitative PCR and promoter-GUS analysis

Total RNA was extracted from the roots, leaves, leaf sheaths, stems and young panicles of 3 month-old cv. Nipponbare wild-type plants, and RNAi transformants, using a RNA prep pure Plant kit (Tiangen Co., Beijing, China), and was reverse transcribed using a SuperScript II kit (TaKaRa), according to

the manufacturers' protocols. An RT-PCR was then conducted based on primer pair cF2/cR2 (targeting *WSL2*) along with the primer pair Actin1F/Actin1R (sequences given in Table S1) targeting the reference gene *ACTIN1*. A quantitative PCR was based on total RNA extracted as above from the leaves of 2 month-old plants. The PCR targeted the following genes: *OsFATB1* (*Os06g0143400*), *OsLACS1* (*Os05g0132100*), *OsCER6* (*Os06g0598800*), *OsKCR1* (*Os04g0483500*), *OsPAS2* (*Os04g0271200*), *OsCER10* (*Os01g0150000*), *OsCER4* (*Os04g0354600*), *OsCER7* (*Os02g0550700*), *OsMAH1* (*Os03g0140100*) and *WSL2* (*Os09g0426800*). The rice ubiquitin gene (*Os03g0234200*) was chosen as a reference gene. The sequences of the relevant primers are given in Table S1. The PCR was based on an SYBR premix Ex TaqTM kit (TaKaRa), following the manufacturer's protocol. The $2^{-\triangle\triangle CT}$method was used to calculate relative changes in gene expression (Livak and Schmittgen 2001).

A promoter GUS assay was based on the 3,391 bp of sequence upstream of *WSL2*, which was amplified by primer pair ProF1/ProR1 (sequences given in Table S1), and the resulting amplicon was cloned into the *Sma*I site of pCAMBIA1305 using a CloneEZ^{TM} PCR Cloning kit (GenScript Co.). The resulting plasmid pWSL2promoter-35S-GUS was digested by *Bgl*II (TaKaRa), and the 35S promoter sequence deleted. The final transformation construct (pWSL2promoter-GUS) was introduced into cv. Kitaake by *A. tumefaciens*-mediated transformation, as above. GUS activity was assayed following Jefferson (1987). The images were obtained using a Leica MZ16 microscope with DFC420 camera (Leica).

Subcellular localization

A 1.86 kb *WSL2* cDNA fragment, amplified by the primer pair gfpF1(XhoI)/gfpR1(SpeI) (sequences given in Table S1), was cloned into the *Xho*I–*Spe*I site of the PA7-GFP vector (Sohlenkamp et al. 2002), and this construct was co-transformed into *A. thaliana* and rice protoplasts using the marker plasmid mCherry-HDEL which contains an ER retrieval tetrapeptide (Chiu et al. 1996; Nelson et al. 2007). The transformed protoplasts were then incubated in the dark at 28°C for 16 h, before being monitored for GFP expression, and observed using a Nikon Eclipse TE2000-U microscope (Nikon Co. Tokyo, Japan).

Results

wsl2 is a cuticular wax mutant

M3-688 was a selection from a screen of 4,000 M_3 lines derived from EMS-treated LTH. Its leaves are light green in appearance, its mature height is somewhat less than that of the wild type, and its self-fertility is around 74%, even though its pollen after iodine staining appeared normal (Fig. S1a–c). The leaves of the mutant displayed a thin film wetting, unlike water droplets forming beads by wild-type leaves. This trait was used as a phenotypic marker during the subsequent map-based cloning exercise (Fig. 1a, b). SEM analysis revealed that substantially fewer cuticular wax crystals were deposited on the surface of the mutant's leaf blade and sheath compared with the wild type (Fig. 1c–h), whereas the outer epidermis waxes on the anther and lemma appeared unaffected (Fig. S1 d–g). The mutant was designated *wsl2* (*wax crystal-sparse leaf2*), following the previously identified wax crystal-sparse leaf mutant *wsl1* (Yu et al. 2008).

wsl2 displays altered cuticle permeability

Cuticle permeability is strongly influenced by the quantity of cuticular wax present. The chlorophyll leaching assay showed that chlorophyll was more readily extracted from *wsl2* leaves than from wild-type ones (Fig. 2a), and the water loss rate from detached leaves was faster in the mutant than in the wild type (Fig. 2b). When the plants were drought stressed, only 5 out of 40 of the mutant seedlings recovered, whereas 36 out of 40 wild-type seedlings survived (Fig. 2c–e). Thus, the *wsl2* cuticle is more permeable than the wild-type one.

wsl2 forms a thicker cuticle membrane

Some *A. thaliana* wax-related mutants display alterations in their cuticle membranes (Chen et al. 2003; Lee et al. 2009; Lu et al. 2009). TEM analysis of three-leaf seedlings showed that the *wsl2* cuticle membrane was somewhat thicker than that of the wild type (Fig. 3a, b). In older plants, this difference became magnified, with the cuticle membrane thickness ranging from 300 to 350 nm in the mutant, but only from 110 to 150 nm in the wild type (Fig. 3c–d). Rather than the compact cuticle proper of the wild type, the mutant cuticle proper had a fluffy appearance and was intermingled with unidentified shadow-stained materials, resulting in the mutant cuticle proper being more fragile and more easily detached from the cuticular layer during sample preparation (Fig. 3d).

Composition of the cuticular wax in *wsl2*

The per area wax content on the *wsl2* leaf blade was 1.68 μg/cm^2, equivalent to ~20% of wild-type content. The most obvious loss of individual wax components were for fatty acids (0.96 μg/cm^2 in *wsl2* vs. 2.86 μg/cm^2 in the

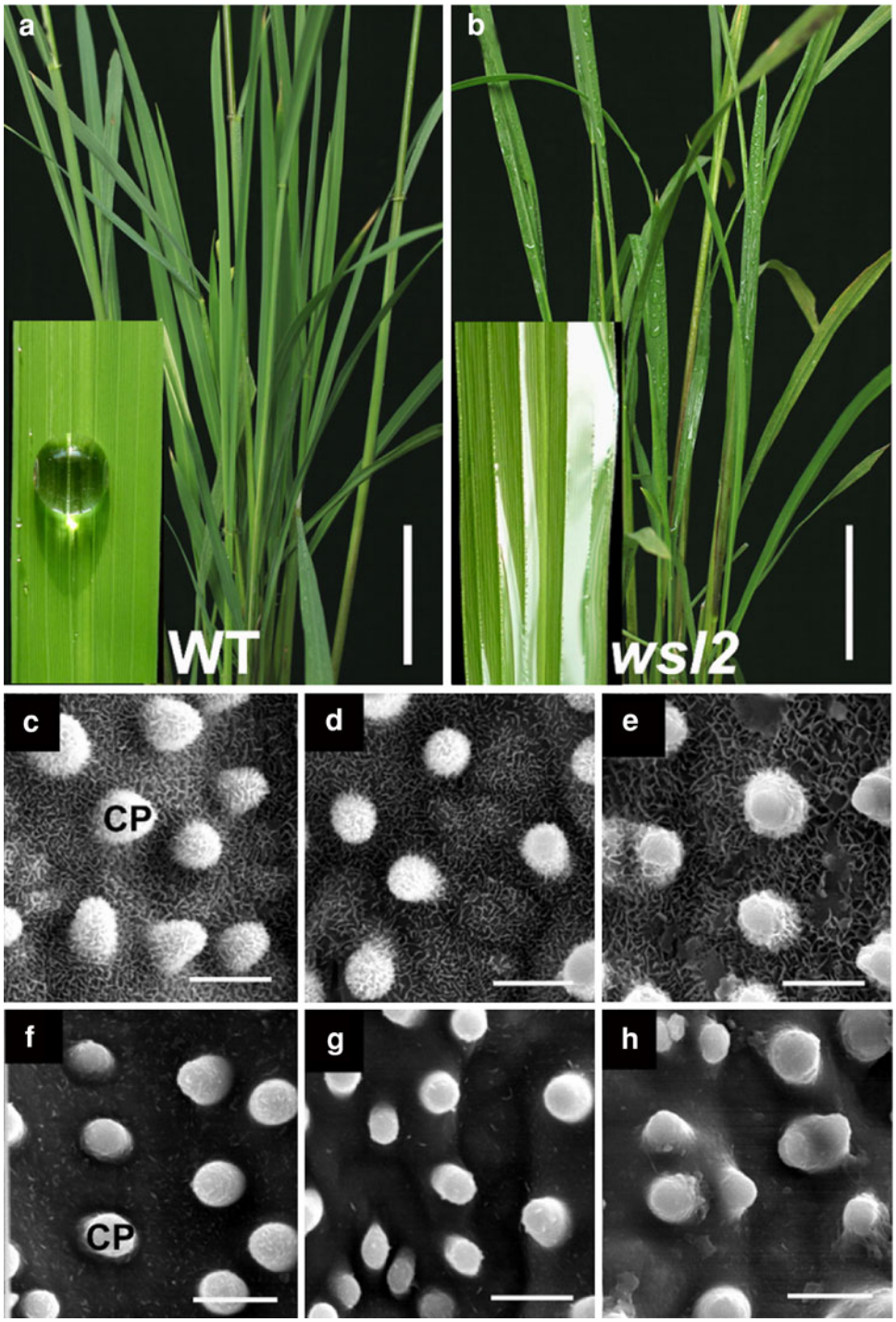

Fig. 1 Phenotype of the rice wild type and the *wsl2* mutant. The behaviour of water droplets on the leaves of wild type (**a**) and *wsl2* (**b**). Cuticular wax formed by wild type (**c**–**e**) and *wsl2* (**f**–**h**), as visualized by SEM, on the adaxial (**c**, **f**) and the abaxial surface (**d**, **g**) of the leaf blade. **e**, **h** Outer epidermis of the leaf sheath. cp cuticular papillae. *Bars* = 10 cm (**a**, **b**), 5 μm (**c**–**h**)

wild type), aldehydes (0.13 vs. 2.60 μg/cm^2), and primary alcohols (0.06 μg vs. 2.00 μg/cm^2). Relative component contents were also altered. The VLCFA precursors represented 34.3% of the overall wax content in the wild type, but 57.4% in the mutant, while the relative contribution of aldehydes fell from 31.2 to 7.9%, and of primary alcohols from 23.9 to 3.4% (Table 1). The leaf sheath wax behaved similarly (Table 1). Each of the individual constituents (C22–C32 fatty acids, C26–C32 primary alcohols, C28–C34 aldehydes and C23–C33 alkanes) was reduced in the mutant compared with the wild type (Fig. 4a, b). Particularly striking was the change in both C30–C32 aldehydes and C30 primary alcohol, which were just 4.8 and 2.2% on the *wsl2* leaf. All the results suggested that, in *wsl2*, the wax constituents decrease both in acyl reduction pathway and alkane-forming pathway.

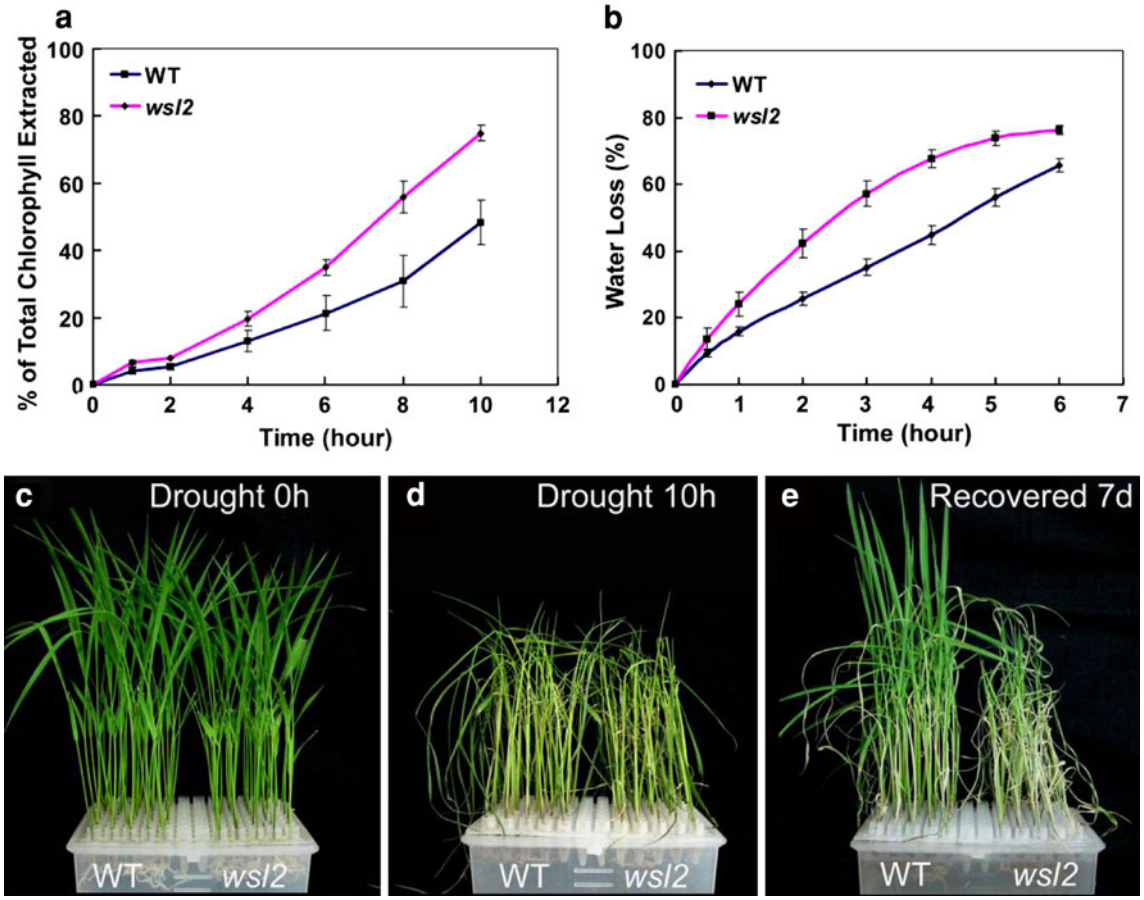

Fig. 2 Physiological characterization of rice wild-type and *wsl2* mutant. **a** Chlorophyll leaching assays with leave of wild-type (WT) and the *wsl2* mutant. **b** Rate of water loss from detached leaves of WT and *wsl2*. The results were obtained from three replicates and depicted with standard error of the mean from each time point. **c**–**e** Drought treatment with the 2 week-old seedlings in the air for 0 h (**c**), 10 h (**d**), seedling recovery 7 days after re-watering (**e**)

Mapping and isolation of *wsl2*

The mutant phenotype segregated in the F_2 mapping population consistently with a 3:1 ratio ($P > 0.05$, $n = 205$) indicating that the mutant phenotype is under the control of a single gene. A map based on a moderate number of progeny placed the *WSL2* locus on the long arm of chromosome 9 in an interval flanked by the microsatellites RM3700 and RM2437. The fine-mapping population narrowed the interval to 30 kb, flanked by the de novo indel markers In 9-1 and In 9-5, both of which are present on BAC clone OJ1299_A11 (Fig. 5a). This interval contains four recognizable open reading frames, one of which (*Os09g0426800*) encodes a protein homologous to WAX2/GL1, and was thus a strong candidate for *WSL2*. The sequence consists of ten exons and nine introns, producing a predicted transcript of length 2,366 bp (AK060786), which is composed of an 1,860 bp coding region, a 158 bp 5′-UTR and a 348 bp 3′-UTR (Fig. 5b). When the 30 kb interval was resequenced in the mutant line, a single base mutation (G to A) was discovered in *Os09g0426800*. The effect of the variant was to lengthen the transcript by 85 bp, since the sixth intron was no longer spliced, and this resulted in the formation of a premature TAA stop codon (Fig. 5b–d). When the 8.33 kb genomic WSL2 DNA fragment (including the 2.12 kb upstream of the ATG start and the 2.27 kb region downstream of the stop codon, was introduced into the wsl2 mutant, the cuticular wax of the transgenic plants resembled that of the wild type (Fig. 5e, f). This result confirms that the single base change in *WSL2* caused the wax crystal sparse leaf phenotype.

RNAi knock-down of wild-type *WSL2*

When the construct containing both the antisense and sense version of a 303 bp 3′UTR fragment of *WSL2* driven by the ubiqutin promoter (Fig. 6a) was introduced into cv. Nipponbare, RT-PCR analysis revealed that *WSL2* expression was disrupted in six of the 21 primary transgenics investigated (Fig. 6b). The leaves of these plants displayed the

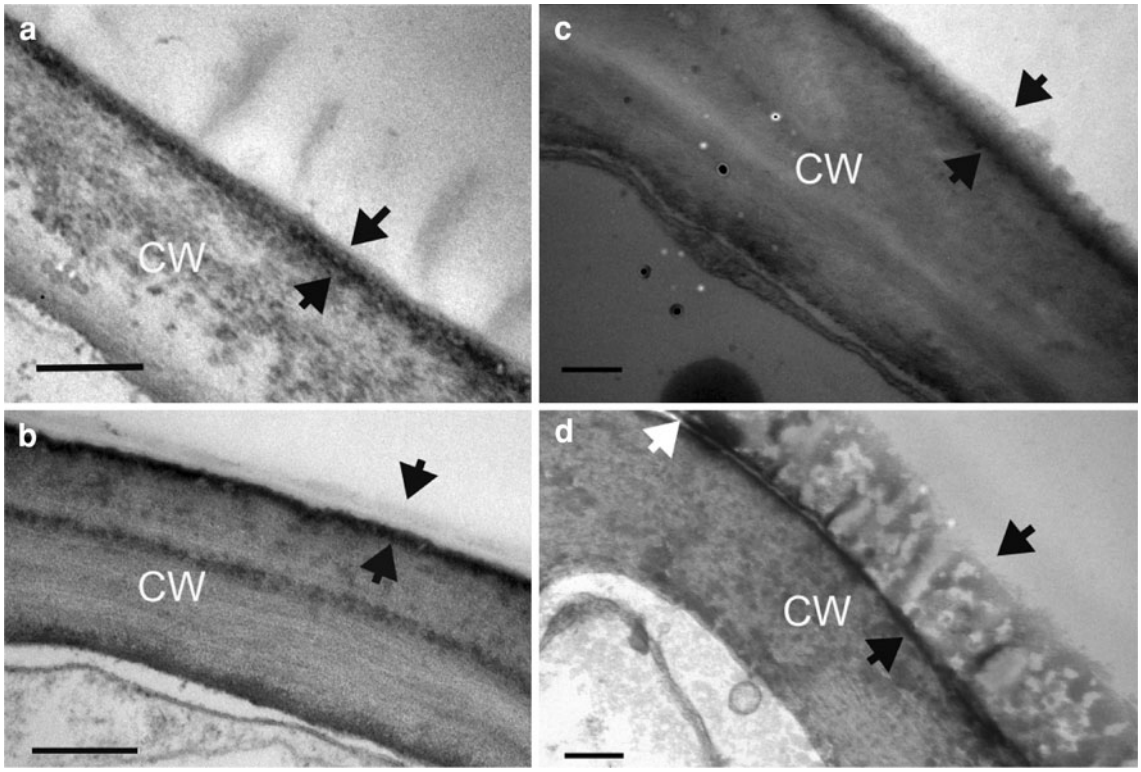

Fig. 3 TEM analysis of leaf cuticle membranes. The leaf cuticle membrane of a wild-type young leaf (**a**) and adult leaf (**c**) comprises the outer electron-translucent cuticle proper and the inner opaque cuticular layer, especially visible in the adult leaf. In the *wsl2* mutant, the young leaf (**b**) and the adult leaf (**d**) cuticle membrane appears thickened and disorganized, especially in the adult leaf. The zone of detachment occurring during sample preparation is indicated by a *white arrowhead* in (**d**). *CW* cell wall. *Bars* = 200 nm

Table 1 Leaf blade and leaf sheath cuticular waxes in the wild-type and the *wsl2* mutant

Compound class	Measurement	Leaf blade		Leaf sheath	
		Wild type	*wsl2*	Wild type	*wsl2*
Fatty acids	Amount	2.86 ± 0.27	0.96 ± 0.17	1.96 ± 0.38	0.85 ± 0.19
	Percentage	34.3 ± 3.2	57.4 ± 10.1	42.6 ± 8.3	66.2 ± 14.5
Aldehydes	Amount	2.60 ± 0.19	0.13 ± 0.03	1.11 ± 0.20	0.07 ± 0.02
	Percentage	31.2 ± 2.3	7.9 ± 2.0	24.1 ± 4.4	5.2 ± 1.3
Primary alcohols	Amount	2.00 ± 0.10	0.06 ± 0.01	1.04 ± 0.11	0.05 ± 0.01
	Percentage	23.9 ± 1.2	3.4 ± 0.3	22.7 ± 2.5	4.2 ± 0.7
Alkanes	Amount	0.58 ± 0.10	0.32 ± 0.04	0.41 ± 0.02	0.25 ± 0.02
	Percentage	6.9 ± 1.2	19.0 ± 2.6	8.9 ± 0.5	19.6 ± 1.2
Esters	Amount	0.31 ± 0.12	0.21 ± 0.03	0.08 ± 0.02	0.06 ± 0.02
	Percentage	3.7 ± 1.4	12.3 ± 2.0	1.7 ± 0.4	4.8 ± 1.4
Total	Amount	8.35 ± 0.78	1.68 ± 0.28	4.60 ± 0.74	1.29 ± 0.25

Mean total wax amount (μg/cm^2 ± SD), total amount of each wax class (μg/cm^2 ± SD), and percentage of each class within each sample extract are shown

mutant phenotype (Fig. 6c, d). SEM analysis of the three RNAi plants R4, R8 and R14 showed that they all had the wax crystal-sparse leaf phenotype (Fig. 6e–h). GC–MS analysis of the cuticular wax present on R4 leaves revealed a two- to fourfold reduction in the content of C24–C30 fatty acids, C28–C34 aldehydes and C26–C32 primary alcohols (Fig. 6i, Table S2). However, unlike in *cer6* mutants (Millar et al. 1999; Fiebig et al. 2000), no shorter product accumulation was found either in *wsl2* or in *WSL2* knock-down transformants.

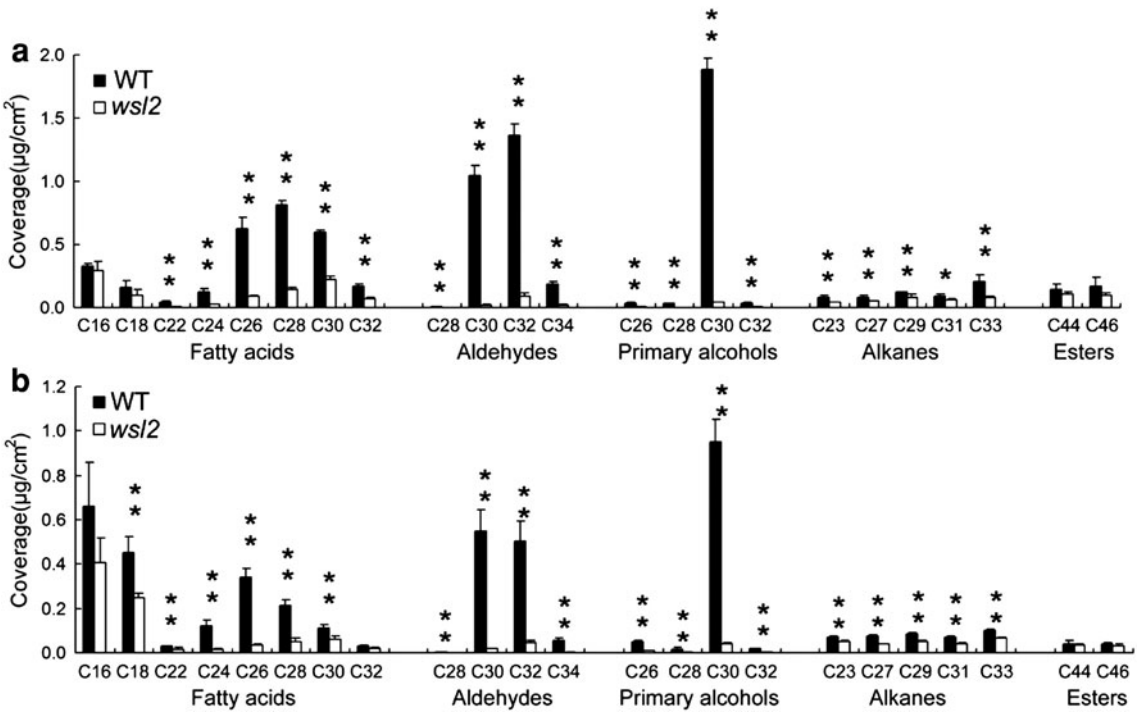

Fig. 4 Cuticular wax composition in the leaf blade (**a**) and the leaf sheath (**b**). *Bars* indicate the mean and standard error from three independent assays. Statistical significance of differences between wild type and *wsl2* means indicated by * ($P < 0.05$) or ** ($P < 0.01$)

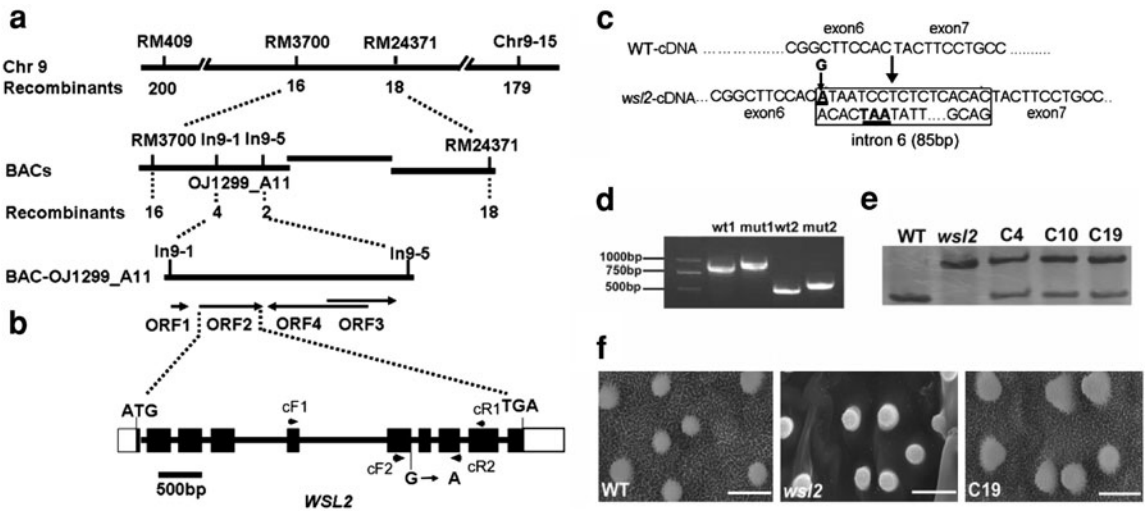

Fig. 5 Positional cloning of *WSL2*. **a** Genetic and physical map, showing the identity of the marker loci and the number of recombinants identified between adjacent markers. **b** The structure of *WSL2*. The mutant allele contains a G to A transition at the first base of the sixth intron. *Black boxes* indicate the coding sequence, *white boxes* the 5′- and 3′-UTRs, and *lines between boxes* introns. The start codon (ATG) and the stop codon (TGA) are both shown. **c** The mutation incorporates the sixth intron into the transcript, introducing a premature TAA termination codon. **d** The mutant transcript as detected by RT-PCR is longer than the corresponding wild-type one. **e–f** Genetic complementation of *wsl2*. **e** A dCAPS marker based on the mutant′s G to A transition identifies transgenic plants. **f** SEM analysis of the leaf of the wild type (*left*), the *wsl2* mutant (*centre*) and a transgenic plant C19, a *wsl2* individual transformed with an 8.33 kb DNA fragment composed of 2.12 kb of sequence upstream of the *WSL2* ATG start codon, the *WSL2* coding sequence and 2.27 kb downstream of the *WSL2* stop codon (*right*). *Bars* = 5 μm

WSL2 is a member of WAX2-like protein family

The WSL2 protein comprises 619 residues with a predicted molecular mass of 69.7 kDa and pI of 9.30. The protein includes four transmembrane domains, as well as a functional domain in both its N-terminal and C-terminal regions. The N-terminal region also contains three His-rich motifs and shares partial homology with a fatty acid

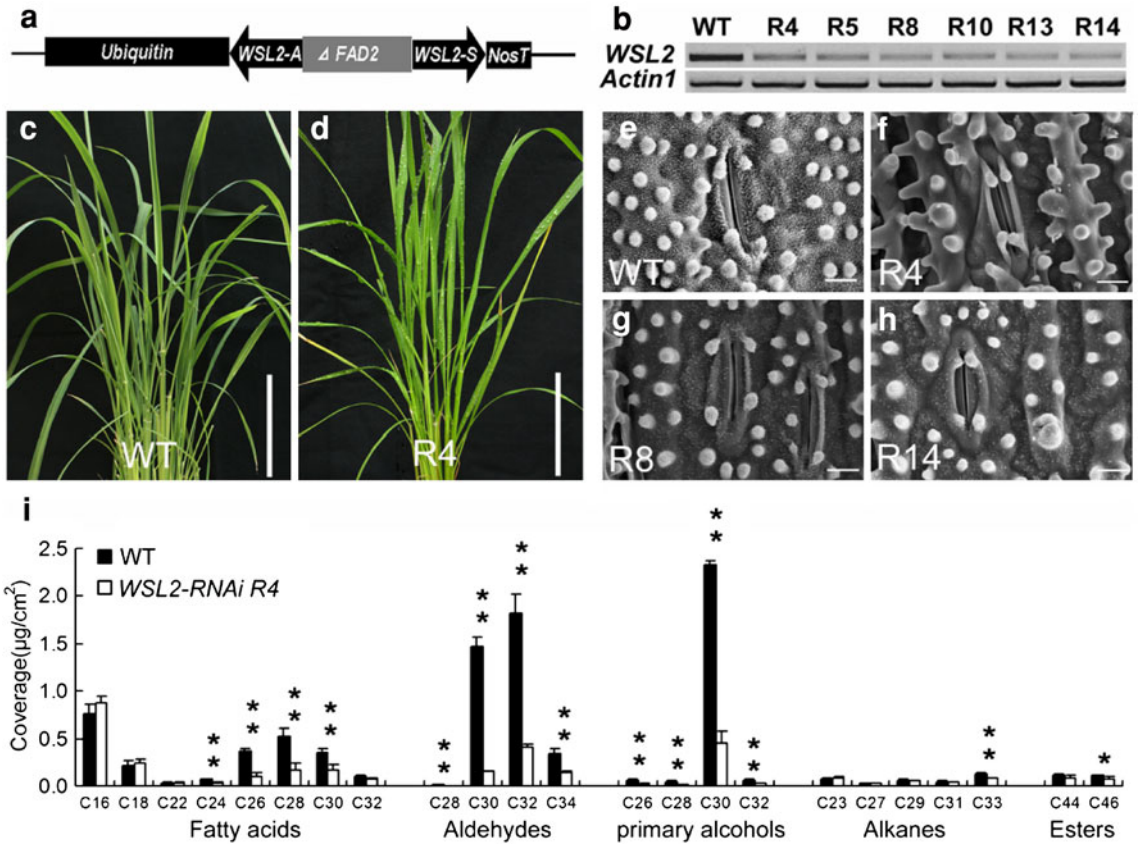

Fig. 6 RNAi knock-down phenotype. **a** Structure of the RNAi construct. **b** Expression of *WSL2*, as assessed by RT-PCR in six transformed plants. **c**, **d** Behaviour of water droplets on the leaf of wild-type and transformant R4. **e**–**h** SEM analysis of wild type and transformants R4, R8 and R14. **i** Constituents of the leaf cuticular wax of wild-type and RNAi knock-down plants. *Bars* indicate the mean and standard deviation error from three independent assays. Statistical significance of differences between wild-type and transgenic plants indicated by *($P < 0.05$) or **($P < 0.01$). *Bars* = 10 cm (**c**, **d**), 5 μm (**e**–**h**)

hydroxylase superfamily involved in cholesterol synthesis and plant cuticular wax synthesis (Arthington et al. 1991). The Wax2_C domain has a conserved LEGW sequence motif with high similarity to short-chain dehydrogenases (Chen et al. 2003). WSL2 shares 85% peptide identity with GL1, and 64 and 37% identity with WAX2 and CER1, respectively (Aarts et al. 1997; Chen et al. 2003; Sturaro et al. 2005). Five WSL2 homologues in rice share 27–69% amino acid identity with WSL2 (Fig. S2a). All 13 proteins showing a substantial level of peptide similarity were classifiable into two clades. The first includes WSL2, GL1, OsGL1-2 (Islam et al. 2009), WAX2, and two sorghum (04g005330, 10g025920) and two maize (LOC100280351, LOC100192547) proteins of unknown function, while the second groups CER1, WDA1 (Jung et al. 2006) and two rice proteins (Os02g0621300, Os04g0512200) of unknown function (Fig. S2b; Table S3).

Expression and intracellular localization of WSL2

RT-PCR analysis of 3 month-old wild-type and mutant plants confirmed that the *WSL2* (or *wsl2*) sequence was strongly expressed in the panicle, leaf and leaf sheath, only weakly in the stem, and not at all in the root (Fig. 7a). The expression of *wsl2* appeared to be enhanced in the leaf of the mutant. As expected, the transcript *wsl2* transcript was longer than the *WSL2* one (Fig. 5b, Fig. 7a). GUS expression, driven by the 3.39 kb fragment upstream of the *wsl2* ATG start, was strong in the glume, leaf blade and sheath, weak in the stem, and undetectable in the root (Fig. 7b–g), fully consistent with the RT-PCR result. Of the ten rice homologues of *A. thaliana* wax synthesis-related genes, four (*OsFATB1*, *OsLACS1*, *OsCER6*, *OsKCR1*) were more highly expressed in the mutant than in the wild type (Fig. 7h).

Most of the wax synthesis-related enzymes in *A. thaliana* are located at the ER (Xu et al. 2002; Zheng et al. 2005; Rowland et al. 2006; Greer et al. 2007). The SignalP 3.0 Server (www.cbs.dtu.dk/services/) predicted the presence of an ER-signalling peptide at the 5′-terminus of the WSL2 protein. The intracellular localization of WSL2 was explored using a GFP fusion construct transiently expressed in both *A. thaliana* and rice leaf protoplasts. The resulting GFP signal co-localized with the ER marker mCherry-HDEL (Nelson et al. 2007; Wang et al. 2010) both in *A. thaliana* (Fig. 8a–d) and rice (Fig. 8e–h)

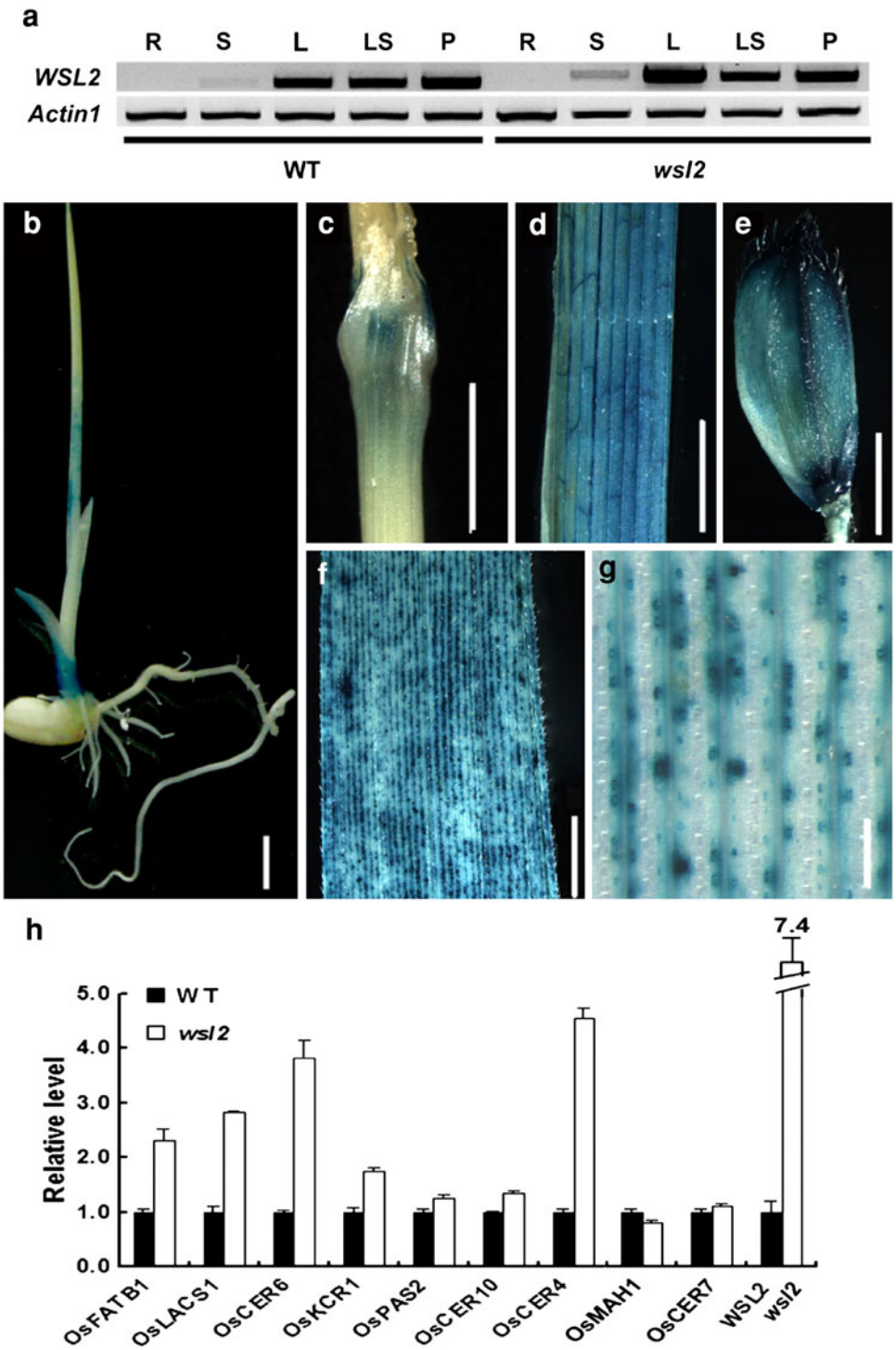

Fig. 7 Expression of *WSL2*. **a** RT-PCR profiles derived from the root (R), stem (S), leaf blade (L), leaf sheath (LS) and panicle (P) of wild-type and the *wsl2* mutant. **b–g** Expression, as detected by a GUS assay in a transgenic plant carrying the *WSL2* promoter fused to *GUS*, in a seedling (**b**), a stem (**c**), a leaf sheath (**d**), a glume (**e**), a leaf blade (**f**), and a leaf blade shown under higher magnification (**g**). **h** Relative expression of a set of genes associated with wax synthesis in the wild-type and the *wsl2* mutant. *Bars* indicate the mean and standard error derived from three independent assays. *Bars* = 1 mm (**b–f**), 0.2 mm (**g**)

protoplasts, supporting the suggestion that WSL2 is targeted to the ER.

Discussion

The three wax-related genes *WSL2*, *WAX2* and *GL1* share a substantial level of homology at the peptide level (85% between WSL2 and GL1, 64% between WSL2 and WAX2). In the *wsl2* mutant, the amount of wax present on the surface of both the leaf blade and leaf sheath is considerably reduced compared with the wild type, with most of the components generated both by the acyl reduction and alkane-forming pathways being affected. The *A. thaliana wax2* mutant has a similar phenotype, with the presence of alkanes, ketones, aldehydes and secondary alcohols being

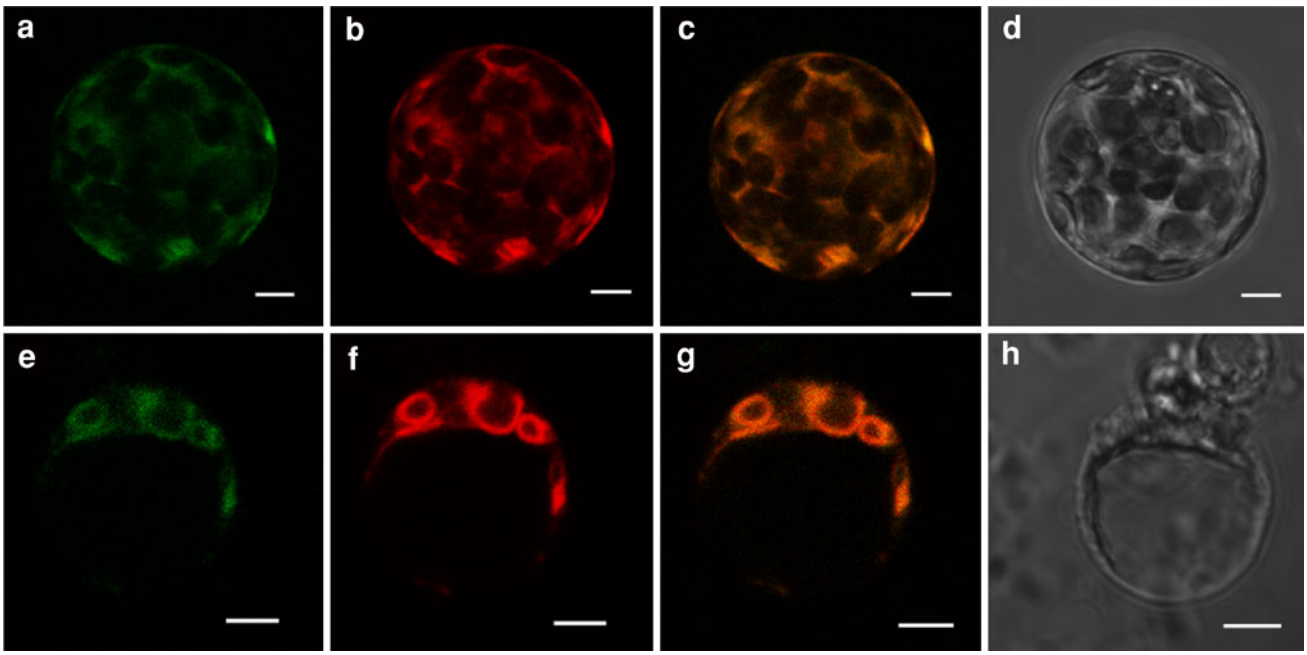

Fig. 8 Intracellular localization of WSL2 in protoplasts of *A. thaliana* (**a**–**d**) and rice (**e**–**h**). **a**, **e** WSL2-GFP on its own. **b**, **f** ER marker mCherry-HDEL. **c** Merged image of **a** and **b**. **g** Merged image of **e** and **f**. **d**, **h** DIC images. *Bars* = 5 μm (**a**–**d**), 4.4 μm (**e**–**h**)

greatly diminished, although that of the C30 primary alcohols on the stem surface is enhanced (Chen et al. 2003). Compared with its wild type, the maize *gl1* mutant produces some 73% less wax on young leaves, largely due to a loss of aldehydes and primary alcohols (Sturaro et al. 2005). The cuticular wax formed on the rice leaf consists mainly of fatty acids, primary alcohols and aldehydes, but in *A. thaliana*, the cuticular wax on the stem is composed of a mixture of alkanes and ketones (of various lengths), with alcohols, aldehydes and fatty acids accounting for less than 25% of the total (Chen et al. 2003). The contrasting composition of cuticular wax between rice and *A. thaliana*, together with the different effect on C30 primary alcohol content caused by the loss of function of *wsl2* and *wax2*, suggests that these two genes do not play exactly the same role in the synthesis of cuticular wax.

In all three mutants (*wsl2*, *wax2* and *gl1*), both the morphology of the cuticle membrane and the composition of the cuticular wax are altered from the wild type (Chen et al. 2003; Sturaro et al. 2005). The *wsl2* leaf cuticle membrane was thickened, in addition to produce a clearly visible demarcation between the cuticle proper and the cuticular layer; in *wax2* the cuticle proper appears thickened, but there was no evidence for a bilayered structure (Chen et al. 2003). A further feature of the *wsl2* mutant is the fact that the cuticle proper becomes easily detached from the cuticular layer during sample preparation. As a result, most of TEM samples lacked the cuticle proper, which created a false impression of the thinness of the cuticle membrane. However, in the *gl1* mutant, the cuticle proper was more or less absent, reducing cuticle membrane thickness by about 50% (Sturaro et al. 2005). The extraction of chlorophyll from *wax2* and *wsl2* leaves is much easier than from those of *gl1*, which behave identically to wild-type leaves (Chen et al. 2003; Sturaro et al. 2005).

In *A. thaliana*, a defective cutin structure is often associated with organ fusion and loss of pollen fertility (Lolle et al. 1998; Pruitt et al. 2000; Wellesen et al. 2001). For example, the *wax2* phenotype includes various abnormalities in trichome development and postgenital organ fusion (Chen et al. 2003; Kurata et al. 2003). However, as in *gl1* (Sturaro et al. 2005), postgenital organ fusion does not occur in *wsl2*. This difference may reflect the closer phylogenetic relationship existing between the two monocotyledonous species maize and rice, than between either of them and the dicotyledonous species *A. thaliana*. The *wsl2* mutant developed normal wax coating on its anthers, and enjoyed a high degree of pollen fertility (although a somewhat reduced rate of grain set), while *wax2* suffers from severe pollen sterility, at least under low relative humidity growing conditions (Chen et al. 2003). The cause of the compromised self fertility of *wsl2* is unclear.

WSL2, WAX2 and GL1 each feature two putative conserved domains, namely a fatty acid hydroxylase superfamily domain in the N-terminal region and a *wax2* C-terminal domain. In addition, they also contain three conserved His-rich motifs. Almost all wax synthesis-related proteins have been localised to the ER (Samuels et al.

2008; Kamigaki et al. 2009), and the pattern of *WSL2* expression is consistent with this (note, however, Qin et al. (2011) reported that the gene product of Os*gl1-1*, which appears to be the same protein as WSL2, is deposited in the nucleus, cytoplasm, and plasma membrane). According to the Kunst and Samuels (2009) model, long-chain (C16–C18) fatty acyl groups are initially synthesized in the plastid, from where they are exported to the ER and extended to VLCFAs by the FAE complex, and then further modified to form the various aliphatic wax components present in the ER. Wax components can be generated either via the alcohol-forming (acyl reduction) pathway (producing primary alcohols and wax esters) or the alkane-forming (decarbonylation) pathway (aldehydes, alkanes, secondary alcohols, and ketones). The elevated level of C30 primary alcohols present in the *wax2* wax was suggested to reflect the encoding by *WAX2* of an enzyme involved in the reduction of aldehyde-generating acyl-CoAs (Chen et al. 2003; Kurata et al. 2003). Compared with the wild type, almost all the components of the *wsl2* wax were reduced in amount. As the defect set in as early as during C22 fatty acid synthesis, the *wsl2* mutation clearly exerted its effect at the initiation stage of the VLCFA elongation process.

The expression of some wax synthesis-related genes differed between the wild-type and the *wsl2* mutant. Apart from the expected reduction in *WSL2* expression, there was an increase of two- fivefold in *OsFATB1*, *OsLACS1*, *OsCER6* and *OsCER4* (Fig. 7h). In *A. thaliana*, *FATB1* and *LACS1* are both thought to participate in the synthesis of <C16 fatty acids precursors (Bonaventure et al. 2003; Lu et al. 2009). A comparison of the wax produced by *wsl2* and wild type showed a similar level of C16 fatty acids, indicating that there was no direct effect of enhanced *OsFATB1* and/or *OsLACS1* expression on short-chain precursor synthesis. The *A. thaliana* FAE complex consists of CER6, AtKCR1, PAS2 and CER10, and in the absence of *CER6* expression stem wax accumulation is abolished (Millar et al. 1999). In *wsl2*, the co-ordinated expression of *OsCER6* and *wsl2* could mean that *wsl2* is a regulator of the rice FAE complex. The wax-deficient phenotype of the *wsl2* mutant is reminiscent of that of various FAE complex gene mutants (Zheng et al. 2005; Bach et al. 2008; Beaudoin et al. 2009), which suggests that *wsl2* has a similar role in VLCFA elongation. However, yeast two-hybrid experiments have not so far succeeded in demonstrating any direct interaction between WSL2 and any of OsCER6, OsKCR1, OsPAS2 or OsCER10 (data not shown), so the control of *WSL2* over the expression of FAE complex genes may rather be indirect. Unexpectedly, *OsCER4* are up-regulated in the *wsl2* mutant. In *Arabidopsis*, *CER4* is responsible for producing primary alcohols (Rowland et al. 2006), but despite of *OsCER4* increased expression, the *wsl2* mutation still blocks accumulation of fatty alcohols. The reason why this kind of apparent paradox happens in *wsl2* need to be further explored in future experiment.

Here, we have shown that WSL2 encodes a protein homologous to *A. thaliana* WAX2 and maize GL1, and is important for the synthesis of cuticular wax and the formation of the cuticle membrane. When the expression of *WSL2* is abolished, the synthesis of almost all the constituents of the wax was decreased. Because shorter product accumulation was found neither in *wsl2* nor in *WSL2* knock-down transformants as in *cer6* mutants (Millar et al. 1999; Fiebig et al. 2000), *WSL2* likely affects utilization of the elongated products in some way; however, its precise function and roles in wax synthesis clearly needs further study.

Acknowledgments We thank for Drs. Xianchun Xia (Institute of Crop Science, CAAS) and Zhigang Zhao (Nanjing Agricultural University) for their critical reading of the manuscript. This research was supported by Grants from the Chinese '973' Program (2007CB10880-1), National Transform Science and Technology Program (2009ZX08009-104B) and National Natural Science Foundation (30871498).

References

Aarts MG, Hodge R, Kalantidis K, Florack D, Wilson ZA, Mulligan BJ, Stiekema WJ, Scott R, Pereira A (1997) The *Arabidopsis* MALE STERILITY 2 protein shares similarity with reductases in elongation/condensation complexes. Plant J 12:615–623

Ariizumi T, Hatakeyama K, Hinata K, Sato S, Kato T, Tabata S, Toriyama K (2003) A novel male-sterile mutant of *Arabidopsis thaliana*, faceless pollen-1, produces pollen with a smooth surface and an acetolysis-sensitive exine. Plant Mol Biol 53:107–116

Arthington BA, Bennett LG, Skatrud PL, Guynn CJ, Barbuch RJ, Uibright CE, Bard M (1991) Cloning, disruption and sequence of the gene encoding yeast C-5 sterol desaturase. Gene 102:39–44

Bach L, Michaelson LV, Haslam R, Bellec Y, Gissot L, Marion J, Da Costa M, Boutin JP, Miquel M, Tellier F, Domergue F, Markham JE, Beaudoin F, Napier JA, Faure JD (2008) The very-long-chain hydroxy fatty acyl-CoA dehydratase PASTICCINO2 is essential and limiting for plant development. Proc Natl Acad Sci USA 105:14727–14731

Barnes JD, Percy KE, Paul ND, Jones P, McLaughlin CK, Mullineaux PM, Creissen G, Wellburn AR (1996) The influence of UV-B radiation on the physicochemical nature of tobacco (*Nicotiana tabacum* L.) leaf surfaces. J Exp Bot 47:99–109

Beaudoin F, Wu X, Li F, Haslam RP, Markham JE, Zheng H, Napier JA, Kunst L (2009) Functional characterization of the *Arabidopsis* β-ketoacyl-coenzyme A reductase candidates of the fatty acid elongase. Plant Physiol 150:1174–1191

Bianchi G, Lupotto E, Russo S (1979) Composition of epicuticular wax of rice, *Oryza sativa*. Cell Mol Life Sci 35:1417–1540

Bonaventure G, Salas JJ, Pollard MR, Ohlrogge JB (2003) Disruption of the *FATB* gene in *Arabidopsis* demonstrates an essential role of saturated fatty acids in plant growth. Plant Cell 15:1020–1033

Chen X, Goodwin SM, Boroff VL, Liu X, Jenks MA (2003) Cloning and characterization of the *WAX2* gene of *Arabidopsis* involved

in cuticle membrane and wax production. Plant Cell 15:1170–1185
Chiu W, Niwa Y, Zeng W, Hirano T, Kobayashi H, Sheen J (1996) Engineered GFP as a vital reporter in plants. Curr Biol 6:325–330
Fiebig A, Mayfield JA, Miley NL, Chau S, Fischer RL, Preuss D (2000) Alterations in *CER6*, a gene identical to *CUT1*, differentially affect long-chain lipid content on the surface of pollen and stems. Plant Cell 12:2001–2008
Greer S, Wen M, Bird D, Wu X, Samuels L, Kunst L, Jetter R (2007) The cytochrome P450 enzyme CYP96A15 is the midchain alkane hydroxylase responsible for formation of secondary alcohols and ketones in stem cuticular wax of *Arabidopsis*. Plant Physiol 145:653–667
Haas K, Brune T, RüCker E (2001) Epicuticular wax crystalloids in rice and sugar cane leaves are reinforced by polymeric aldehydes. J Appl Bot 75:178–187
Hiei Y, Ohta S, Komari T, Kumashiro T (1994) Efficient transformation of rice (*Oryza sativa* L.) mediated by *Agrobacterium* and sequence analysis of the boundaries of the T-DNA. Plant J 6:271–282
Hooker TS, Lam P, Zheng H, Kunst L (2007) A core subunit of the RNA-processing/degrading exosome specifically influences cuticular wax biosynthesis in *Arabidopsis*. Plant Cell 19:904–913
Islam MA, Du H, Ning J, Ye H, Xiong L (2009) Characterization of *Glossy1*-homologous genes in rice involved in leaf wax accumulation and drought resistance. Plant Mol Biol 70:443–456
Jefferson RA (1987) Assaying chimeric genes in plants: the *GUS* gene fusion system. Plant Mol Biol Rep 5:387–405
Jenks MA, Rich PJ, Peters PJ, Axtell JD, Ashworth EN (1992) Epicuticular wax morphology of *bloomless* (bm) mutants in *Sorghum bicolor*. Int J Plant Sci 153:311–319
Jenks MA, Joly RJ, Peters PJ, Rich PJ, Axtell JD, Ashworth EN (1994) Chemically induced cuticle mutation affecting epidermal conductance to water vapor and disease susceptibility in *Sorghum bicolor* (L.) Moench. Plant Physiol 105:1239–1245
Joubes J, Raffaele S, Bourdenx B, Garcia C, Laroche-Traineau J, Moreau P, Domergue F, Lessire R (2008) The VLCFA elongase gene family in *Arabidopsis thaliana*: phylogenetic analysis, 3D modelling and expression profiling. Plant Mol Biol 67:547–566
Jung KH, Han MJ, Lee DY, Lee YS, Schreiber L, Franke R, Faust A, Yephremov A, Saedler H, Kim YW, Hwang I, An G (2006) *Wax-deficient anther1* is involved in cuticle and wax production in rice anther walls and is required for pollen development. Plant Cell 18:3015–3032
Kamigaki A, Kondo M, Mano S, Hayashi M, Nishimura M (2009) Suppression of peroxisome biogenesis factor 10 reduces cuticular wax accumulation by disrupting the ER network in *Arabidopsis thaliana*. Plant Cell Physiol 50:2034–2046
Kunst L, Samuels L (2009) Plant cuticles shine: advances in wax biosynthesis and export. Curr Opin Plant Biol 12:721–727
Kurata T, Kawabata-Awai C, Sakuradani E, Shimizu S, Okada K, Wada T (2003) The *YORE–YORE* gene regulates multiple aspects of epidermal cell differentiation in *Arabidopsis*. Plant J 36:55–66
Lee SB, Go YS, Bae HJ, Park JH, Cho SH, Cho HJ, Lee DS, Park OK, Hwang I, Suh MC (2009) Disruption of glycosylphosphatidylinositol-anchored lipid transfer protein gene altered cuticular lipid composition, increased plastoglobules, and enhanced susceptibility to infection by the fungal pathogen *Alternaria brassicicola*. Plant Physiol 150:42–54
Li F, Wu X, Lam P, Bird D, Zheng H, Samuels L, Jetter R, Kunst L (2008) Identification of the wax ester synthase/acyl-coenzyme A: diacylglycerol acyltransferase WSD1 required for stem wax ester biosynthesis in *Arabidopsis*. Plant Physiol 148:97–107
Livak KJ, Schmittgen TD (2001) Analysis of relative gene expression data using real-time quantitative PCR and the 2(-Delta Delta C(T)) method. Methods 25:402–408
Lolle SJ, Berlyn GP, Engstrom EM, Krolikowski KA, Reiter WD, Pruitt RE (1997) Developmental regulation of cell interactions in the *Arabidopsis fiddlehead-1* mutant: a role for the epidermal cell wall and cuticle. Dev Biol 189:311–321
Lolle SJ, Hsu W, Pruitt RE (1998) Genetic analysis of organ fusion in *Arabidopsis thaliana*. Genetics 149:607–619
Lu S, Song T, Kosma DK, Parsons EP, Rowland O, Jenks MA (2009) *Arabidopsis CER8* encodes long-chain acyl-CoA synthetase 1 (LACS1) that has overlapping functions with LACS2 in plant wax and cutin synthesis. Plant J 59:553–564
McCouch SR, Teytelman L, Xu Y, Lobos KB, Clare K, Walton M, Fu B, Maghirang R, Li Z, Xing Y, Zhang Q, Kono I, Yano M, Fjellstrom R, DeClerck G, Schneider D, Cartinhour S, Ware D, Stein L (2002) Development and mapping of 2240 new SSR markers for rice (*Oryza sativa* L.). DNA Res 9(Supplement): 257–279
Millar AA, Clemens S, Zachgo S, Giblin EM, Taylor DC, Kunst L (1999) *CUT1*, an *Arabidopsis* gene required for cuticular wax biosynthesis and pollen fertility, encodes a very-long-chain fatty acid condensing enzyme. Plant Cell 11:825–838
Nelson BK, Cai X, Nebenfuhr A (2007) A multicolored set of in vivo organelle markers for co-localization studies in *Arabidopsis* and other plants. Plant J 51:1126–1136
Pruitt RE, Vielle-Calzada JP, Ploense SE, Grossniklaus U, Lolle SJ (2000) *FIDDLEHEAD*, a gene required to suppress epidermal cell interactions in *Arabidopsis*, encodes a putative lipid biosynthetic enzyme. Proc Natl Acad Sci USA 97:1311–1316
Qin BX, Tang D, Huang J, Li M, Wu XR, Lu LL, Wang KJ, Yu HX, Chen JM, Gu MH, Cheng ZK (2011) Rice *OsGL1-1* is involved in leaf cuticular wax and cuticle membrane. Mol Plant doi: 10.1093/mp/ssr1028
Raven JA, Edwards D (2004) Physiological evolution of lower embryophytes: adaptations to the terrestrial environment. In: Hemsley AR, Poole I (eds) The evolution of plant physiology. Elsevier, Oxford, pp 17–41
Riederer M (2006) Introduction: biology of the plant cuticle. Biology of the plant cuticle. Blackwell, Oxford, pp 1–8
Rowland O, Zheng H, Hepworth SR, Lam P, Jetter R, Kunst L (2006) *CER4* encodes an alcohol-forming fatty acyl-coenzyme A reductase involved in cuticular wax production in *Arabidopsis*. Plant Physiol 142:866–877
Rowland O, Lee R, Franke R, Schreiber L, Kunst L (2007) The *CER3* wax biosynthetic gene from *Arabidopsis thaliana* is allelic to *WAX2/YRE/FLP1*. FEBS Lett 581:3538–3544
Samuels L, Kunst L, Jetter R (2008) Sealing plant surfaces: cuticular wax formation by epidermal cells. Annu Rev Plant Biol 59:683–707
Schnurr J, Shockey J, Browse J (2004) The acyl-CoA synthetase encoded by *LACS2* is essential for normal cuticle development in *Arabidopsis*. Plant Cell 16:629–642
Sieber P, Schorderet M, Ryser U, Buchala A, Kolattukudy P, Métraux JP, Nawrath C (2000) Transgenic *Arabidopsis* plants expressing a fungal cutinase show alterations in the structure and properties of the cuticle and postgenital organ fusions. Plant Cell 12:721–738
Sohlenkamp C, Wood CC, Roeb GW, Udvardi MK (2002) Characterization of *Arabidopsis* AtAMT2, a high-affinity ammonium transporter of the plasma membrane. Plant Physiol 130:1788–1796
Stoutjesdijk PA, Singh SP, Liu Q, Hurlstone CJ, Waterhouse PA, Green AG (2002) hpRNA-mediated targeting of the *Arabidopsis FAD2* gene gives highly efficient and stable silencing. Plant Physiol 129:1723–1731

Sturaro M, Hartings H, Schmelzer E, Velasco R, Salamini F, Motto M (2005) Cloning and characterization of *GLOSSY1*, a maize gene involved in cuticle membrane and wax production. Plant Physiol 138:478–489

Taiz L, Zeiger E (1998) Plant defenses: surface protectants and secondary metabolites. Plant physiology, 2nd edn. Sinauer Associates, Sunderland, pp 342–376

Walton TJ (1990) Waxes, cutin and suberin. Methods Plant Biochem 4:5–158

Wang Y, Ren Y, Liu X, Jiang L, Chen L, Han X, Jin M, Liu S, Liu F, Lv J, Zhou K, Su N, Bao Y, Wan J (2010) OsRab5a regulates endomembrane organization and storage protein trafficking in rice endosperm cells. Plant J 64:812–824

Wellesen K, Durst F, Pinot F, Benveniste I, Nettesheim K, Wisman E, Steiner-Lange S, Saedler H, Yephremov A (2001) Functional analysis of the *LACERATA* gene of *Arabidopsis* provides evidence for different roles of fatty acid ω-hydroxylation in development. Proc Natl Acad Sci USA 98:9694–9699

Wu Z, Zhang X, He B, Diao L, Sheng S, Wang J, Guo X, Su N, Wang L, Jiang L, Wang C, Zhai H, Wan J (2007) A chlorophyll-deficient rice mutant with impaired chlorophyllide esterification in chlorophyll biosynthesis. Plant Physiol 145:29–40

Xu X, Dietrich CR, Lessire R, Nikolau BJ, Schnable PS (2002) The endoplasmic reticulum-associated maize GL8 protein is a component of the acyl-coenzyme A elongase involved in the production of cuticular waxes. Plant Physiol 128:924–934

Yu D, Ranathunge K, Huang H, Pei Z, Franke R, Schreiber L, He C (2008) *Wax Crystal-Sparse Leaf1* encodes a beta-ketoacyl CoA synthase involved in biosynthesis of cuticular waxes on rice leaf. Planta 228:675–685

Zheng H, Rowland O, Kunst L (2005) Disruptions of the *Arabidopsis* enoyl-CoA reductase gene reveal an essential role for very-long-chain fatty acid synthesis in cell expansion during plant morphogenesis. Plant Cell 17:1467–1481